American Journal of Physics and Applications
2015; 3(2): 33-38
Published online March 4, 2015 (http://www.sciencepublishinggroup.com/j/ajpa)
doi: 10.11648/j.ajpa.20150302.14
ISSN: 2330-4286 (Print); ISSN: 2330-4308 (Online)

Phase Formation and Crystallinity-Dependent Magnetic Parameters of $Co_{1-x}Fe_{2+x}O_4$ Nanoparticals

Nahed Makram Eyssa, Hanan Hassan Hantour*, Kamilia Sdeek Abdo

Physics Department, Faculty of Science, Girls Branch, Al-Azhar University, Cairo, Egypt

Email address:
Nahedmakrm74@gmail.com (N. M. Eyssa), hananhantourmy@yahoo.com (H. H. Hantour), kamiliasedeek@yahoo.com (N. M. Eyssa)

To cite this article:
Nahed Makram Eyssa, Hanan Hassan Hantour, Kamilia Sdeek Abdo. Phase Formation and Crystallinity-Dependent Magnetic Parameters of $Co_{1-x}Fe_{2+x}O_4$ Nanoparticals. *American Journal of Physics and Applications*. Vol. 3, No. 2, 2015, pp. 33-38.
doi: 10.11648/j.ajpa.20150302.14

Abstract: Nano crystalline cobalt ferrite $CoFe_2O_4$ powders were synthesized using the coprecipitation method. The effect of the calcination temperature and the Fe^{3+}/Co^{2+} molar ratio on the phase formation, macro and microstructure and magnetic properties was studied systematically. The Fe^{3+}/Co^{2+} was controlled to equal 2 and 2.75 while the annealing temperature (T_a) was adjusted to vary from 600 to 1000C°. the obtained powders were investigated using x-ray diffraction (XRD) analysis, Field emission scanning electron microscope (FESEM), Fourir transformation infrared spectroscopy (FTIR) and vibrating sample magnetometer (VSM). For both the Fe^{3+}/Co^{2+} ratios, the XRD results indicat the formation of well crystallized cubic spinel cobalt ferrite phase for the precursors annealed at 600C° up to 1000C°. However a second rhombohedral hematite phase whose content varies respectively from 3% and 15% was formed as the Fe^{3+}/Co^{2+} varied from 2 to 2.75 at T_a=800 and 1000C°. The crystallite size ($\mathcal{D}_\beta$) as determined applying the win-fit program was found also to decrease from 54.5 to 48.6nm accompanied by an increase of the root mean square strain $<\varepsilon_g>$. Using Rditveld analysis no effect on the value of the lattice parameter (a) was detected. The FESEM micrographs reveal the formation of highly agglomerated particles for Fe^{3+}/Co^{2+} =2.75 and T_a =1000C°. The FTIR analysis confirm the formation of the spinel structure phase for both Fe^{3+}/Co^{2+} ratios at 1000C°, however the absorption bands shift to higher frequencies for Fe^{3+}/Co^{2+} =2.75. Other bands at 1663 and 3472cm^{-1} ascribed to free or absorbed water molecules were also detected for this ratio. The Fe^{3+}/Co^{2+} molar ratio was found to have a significant effect on the magnetic properties of the produced cobalt ferrite. The calculated magnetic parameters: the saturation magnetization (M_S= 71.219emu/g), the coricivity (H_C= 1443.8Oe) and the remanence ratio (M_r/M_S= 0.405) were recorded to decrease as the Fe^{3+}/Co^{2+} increases except for the curie temperature (T_C) which increase from 405 to 410C°.

Keywords: Co Ferrite, Synthesized Using the Coprecipitation Method, Structure & Microstructure, Confirm the Formation of the Functional Groups of the Ferrite Structure and Magnetic Properties

1. Introduction

Recently metal-oxide nanoparticles have been the subject of much interest because of their unusual optical, electronic and magnetic properties, which often differ from the bulk.

Spinels of the type $A^{2+}B^{3+}{}_2O_4$ such as $ZnFe_2O_4$, $MnFe_2O_4$, $NiFe_2O_4$ and $CoFe_2O_4$ have attracted considerable attentions due to their broad applications in several technological fields including electronic devices, ferrofluids, magnetic drug delivery, microwave devices and high-density information storage [1–4]. Among spinel ferrites, cobalt ferrite, $CoFe_2O_4$ is especially interesting owing to its magnetic properties such as strong anisotropy, high coercivity at room temperature and moderate saturation magnetization, good mechanical and chemical stability[5,6]. It is also a photomagnetic material that shows light-induced coercivity change[7,8].The most important applications of $CoFe_2O_4$ in technology based on nanosize are high density recording, spintronics, magnetic resonance imaging, magneto refrigeration, ferrofluids, photonic crystals, drug-delivery technology, etc. [9–13].

In a spinel structured compound (AB_2O_4), the unit cell contains 32 oxygen atoms in cubic close packing with 8 tetrahedral (A) and 16 octahedral (B) occupied sites. Magnetization of spinel ferrites originates from difference in the magnetic moments of the cations distributed at tetrahedral A and octahedral B sites and this depends on the super exchange interactions through oxygen as JAB (A–O–B), JAA

(A–O–A) and JBB (B–O–B)[14–16]. When JAB is the strongest interaction, ferrimagnetism occurs. Among the ferrospinels, the inverse type is particularly interesting due to its high magneto-crystalline anisotropy, high saturation magnetization, and unique magnetic structure[17].

In fact, the physical properties of $CoFe_2O_4$ are critically dependent on synthesis technique. Many preparation methods for $CoFe_2O_4$ nanoparticles have been quite involved requiring special techniques to prevent agglomeration [18] or microwave assisted synthesis [19]. Among these synthesis methods are: the wet chemical coprecipitation[20], microwave irradiation in polyol media[21], sol-gel auto-combustion[22], poly ethylene glycol-assisted hydrothermal method[23], mechanical milling and subsequent annealing[24] etc----. Evidently, each method controls the degree of crystallinity, the particle size and the magnetic properties.

The present work is detailed investigation of the structural and magnetic properties of $Co_{1-x}Fe_{2+x}O_4$ (x= 0.0, 0.2). Evolution and characterization tools including x-ray diffraction, Field Emission Scanning Electron Microscope, Fourier Transform InfraRed and Vibration Sample Magnetometer were used. The effect of the Fe^{3+}/Co^{2+} ratio and annealing temperature on the phase formation and crystallinity consequently, on the magnetic parameters were carefully studid.

2. Experimental Procedure

Ferric chloride and cobalt chloride (98 +% purity) and sodium hydroxide were used. All the materials were reagent grade and used without further purification. Double distilled, deionized water was used as a solvent. Two ingots of cobalt ferrite with chemical compositions: $CoFe_2O_4$ and $Co_{0.8}Fe_{2.2}O_4$ were prepared. 0.4M (25 ml) solution of iron chloride and a 0.2M (25 ml) of cobalt chloride solutions were mixed in double distilled, de-ionized water. Deionized distilled water was used as a solvent in order to avoid the production of impurities in the final product. Under vigorously stirring with constant speed using magnetic stirrer, the suspension was kept stirred for 3h at 150C^o. 3M (25 ml) solution of sodium hydroxide was prepared and slowly added to the salt solution dropwise. While dropping, precipitation occurred immediately and the color of the suspension changed to dark brown until PH level of (11-12) was reached. This reaction time was sufficient for dehydration and atomic rearrangement to take place during the conversion of the hydroxides into the ferrite compound. The precipitates were then separated by a high-speed centrifuge at 8000rpm for 8min. To get free particles from sodium and chlorine compounds, the precipitate was then washed 5 times with distilled water then with ethanol to remove the excess surfactant. The precipitate was then dried overnight at 100 C^o. The acquired substance was then grinded into a fine powder. In order to produce nanocrystallites with higher crystallinity and bigger particle size, the as prepared $CoFe_2O_4$ and $Co_{0.8}Fe_{2.2}O_4$ nanocrystals (precipitated at 150C^o) were calcinated at different temperatures 600C^o, 800C^o and 1000C^o each for 7 days.

In order to investigate the structural and the microstructure, the two systems under study were subjected to X-ray diffraction analysis using Cu K_α radiation. The X-ray diffractometr used is a Philips x' pert MPP diffractometr with a goniometer type PW3050/10 with Cu Kα radiation (λ = 1.5418A^o). To reduce preferred orientation the following two steps were considered: first, the material was reduced to a fine state by grinding in agate mortar. This step also reduces the errors arising from the micro absorption effects. Second, back-loading was used for packing the samples. Field Emission Scanning Electron Microscope (Model JEOL, Japan) was used to investigate the surface morphology of the sample. Fourier transform Infra Red was applied to confirm the formation of the functional groups of the ferrite structure. The magnetic properties were measured using a vibrating sample magnetometer at room temperature under a maximum field up to 20 kOe. The magnetization was measured as a function of temperature and the Curie temperature T_C were detected for the two systems.

3. Results and Discussion

3.1. Structural and Microstructral Analysis

3.1.1. XRD Analysis

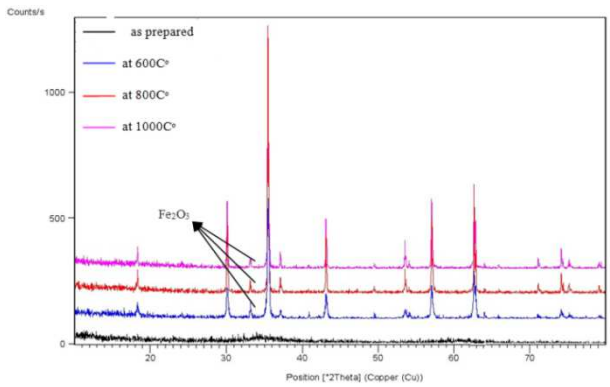

Fig. 1. *Diffraction patterns of $CoFe_2O_4$ as prepared and annealed at different temperatures, each for 7 days.*

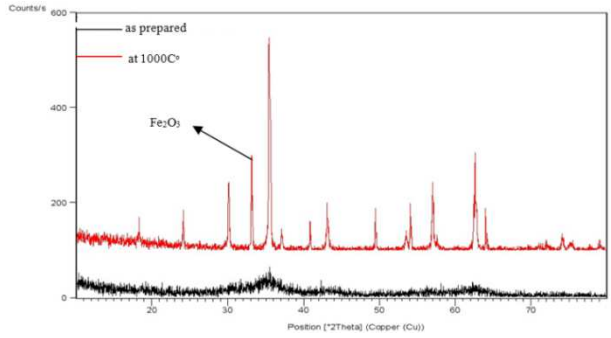

Fig. 2. *Diffraction patterns of $Co_{0.8}Fe_{2.2}O_4$ as prepared and annealed at 1000C^o for 7days.*

Structural studies means to detect the locations of the atoms in the unit cell while microstructural means to find the

crystallite size, strain and type of defects. The XRD patterns of the $CoFe_2O_4$ as prepared and annealed at 600, 800 and 1000C^o are given in Fig.1. Except for the as prepared sample, the patterns reveal that the diffraction line corresponding to the characteristic peaks of cubic spinel type lattice appeared. Application of the search match program confirmed the formation of the cubic spinel structure. Evidently, annealing at 600C^o converts the texture of the as prepared sample to a well defined crystalline state. This degree was sufficient to produce spinel phase with sharpened narrow peaks. However annealing at 800 and 1000C^o produces more intensive peaks reflecting higher degree of crystallinity. Fig.1 shows also some diffraction lines due to the presence of Fe_2O_3 as a second minor phase. The content of hematite as calculated by MAUD program decreases from 5% to 3% as the annealing temperature increases from 600C^o to 800C^o. Higher annealing at 1000C^o has no affect on the Fe_2O_3 content. Similar results of $CoFe_2O_4$ synthesized using organic acid precursor method calcinated between 600C^o and 800C^o show spinel structure with a minor impurity of hematite. XRD study of $CoFe_2O_4$ sintered by conventional ceramic method also confirmed the presence of 13.1% hematite residual phas[25]. The experimental XRD patterns of Fig.1 was found to match well with the specific ICDD card number (04-01-1893) confirming the formation of cubic structure with space group Fd-3m and lattice parameter a = 8.38256A^o. Good reliability factors (R_{wp}% and R_b%) were obtained while calculating the structure parameters.

Similar annealing procedures were carried out for the $Co_{0.8}Fe_{2.2}O_4$ sample. Fig.2 shows the XRD patterns for the as prepared and annealed $Co_{0.8}Fe_{2.2}O_4$ sample (1000C^o). No effect due to the excess of Fe was detected for the (a) value of the spnil phase, however, a large content of Fe_2O_3 (15%) was formed. Other studies on $Co_{0.8}Fe_{2.2}O_4$ reported values of 32.9% for the second phase[26]. The structure of the Fe_2O_3 phase was identified using the ICDD card number (00-033-0664) which gives Rhombohedral structure with space group R-3C and lattice parameters a= 5.0267Å and c= 13.678Å.

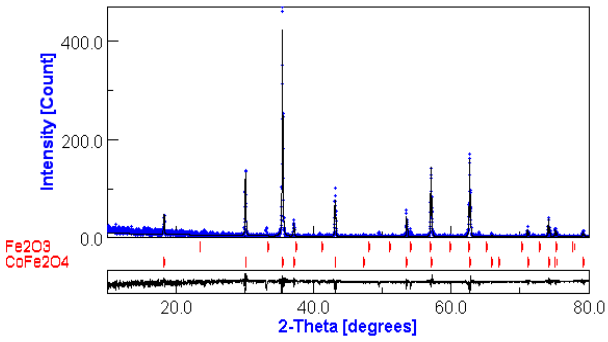

Fig. 3. *The profile fitting of $CoFe_2O_4$ annealed at 1000C^o for 7 days.*

Fig.3 shows, as example, the profile fitting of the $CoFe_2O_4$ system annealed at 1000C^o for 7 days. The refined structural parameters were obtained from Rietveld refinement applying the MAUD program [27] for $CoFe_2O_4$ and $Co_{0.8}Fe_{2.2}O_4$ annealed at 1000C^o. The usual sequence of parameters refinement are: the scale factor, the zero shift and background parameters, lattice parameters, peak profile parameters (size and strain), atoms position and occupancy and finally the displacement parameters.

Table 1. *Apparent crystallite size $\mathcal{D}_\beta$(nm) & $\mathcal{D}_F$(nm) and mean-square strain $< e_g >$ from single and multiple line analysis of the $CoFe_2O_4$ sample annealed at 1000C^o for 7day.*

$CoFe_2O_4$				Fe2O3		
hkl	**single line D_β(nm)**	**analysis D_F(nm)**	**multiple order (hhh)$<e_g>$**	**hkl**	**single line D_β(nm)**	**analysis D_F(nm)**
111	41.8	74.9	0.0041	104	56.1	72.1
220	74.9	87.0		024	59.8	79.0
311	57.1	91.5				
222	59.4	81.3				
400	39.5	75.3				
422	47.7	80.5				
511	74.2	81.3				
440	56.7	66.3				
533	39	84.6				
Aver.	54.5	80.3			57.9	75.5

Table 2. *Apparent crystallite size $\mathcal{D}_\beta$(nm) & $\mathcal{D}_F$(nm) and mean-square strain $< e_g >$ from single and multiple line analysis of the $Co_{0.8}Fe_{2.2}O_4$ sample annealed at 1000C^o for 7 days.*

$Co_{0.8}Fe_{2.2}O_4$				Fe2O3		
hkl	**single line D_β(nm)**	**analysis D_F(nm)**	**multiple order (hhh)$<e_g>$**	**hkl**	**single line D_β(nm)**	**analysis D_F(nm)**
111	42.0	69.4	0.0172	012	51.0	60.1
220	53.6	65.0		104	68.7	77.9
311	48.1	61.9		113	52.2	75.7
222	50.6	52.8		024	50.4	79.7
400	50.0	51.9		300	56.1	82.5
422	42.4	75.4				
511	53.7	63.4				
440	36.3	37.8				
533	61.3	64.0				
Aver.	48.6	60.2			55.7	75.2

Applying the win-fit program, the resulting apparent crystallite size $\mathcal{D}_\beta$(nm) & $\mathcal{D}_F$(nm) and root mean square strain $< e_g >$ from single and multiple line analysis are given in table 1 and 2 for the two detected phase.

Table 3. Summarizes, the effect of increasing the Fe content on the expense of Co. As can be realized, the formation of hematite phases largely increased from 3% to 15% as Fe/Co increased from 2 to 2.75. Smaller crystallite size and higher root mean square strain were also obtained. It is known that defects such as stacking inside the materials which accordingly produce microstrains[28,29]. The higher value of $< e_g >$ for Fe/Co=2.72 reflects higher degree of defect concentration.

Table 3. *Phase formation, average crystallite size (nm), strain, refined lattice parameter a (Å), the reliability factors R_{wp}% and R_p% for the two systems under study.*

Sample	**Fe/Co molar ratio**	**% formed Fe_2O_3**	**Averaged D_β(nm)**	**$< e_g >$**	**a Å**	**R_{wp}**	**R_p**
$CoFe_2O_4$	2:1	3	54.5	$4.1x10^{-3}$	8.38256	4.4	3.7
$Co_{0.8}Fe_{2.2}O_4$	2.75:1	15	48.6	$1.7x10^{-2}$	8.38256	10.6	6.7

3.1.2. Field Emission Scanning Electron Microscope Analysis

Fig.4 displays the FESEM graph of $CoFe_2O_4$ annealed at 1000C°. The image shows spherically shaped crystallites with narrow size distribution (40-51nm). Although the nano particles are dense and distributed regularly over the whole surface, a clear boundary between crystallites can yet be observed. The values of particle size derived from FESEM are in reasonable agreement with those calculated from XRD single line analysis ($\mathcal{D}_\beta$= 54.5nm).

For $Co_{0.8}Fe_{2.2}O_4$ (Fe:Co=2.75), the FESEM graph shows a uniform distribution of elongated particles allover the sample. The apparent size of these agglomeration ranges between 112 and 164nm. Agglomeration is understood to increase because of the interfacial surface tension, which may arise from the magnetostatic or exchange interactions between particles. The formation of 15% hematite in cobalt ferrite matrix also, seems to enhance the agglomeration process.

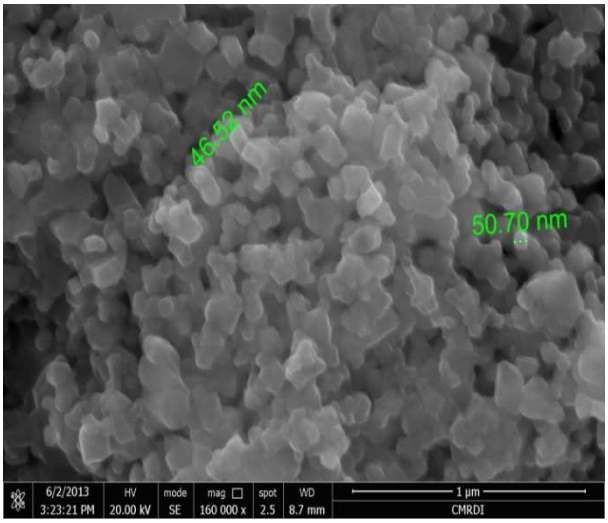

Fig. 4. *FESEM micrograph of the $CoFe_2O_4$ annealed at 1000C°.*

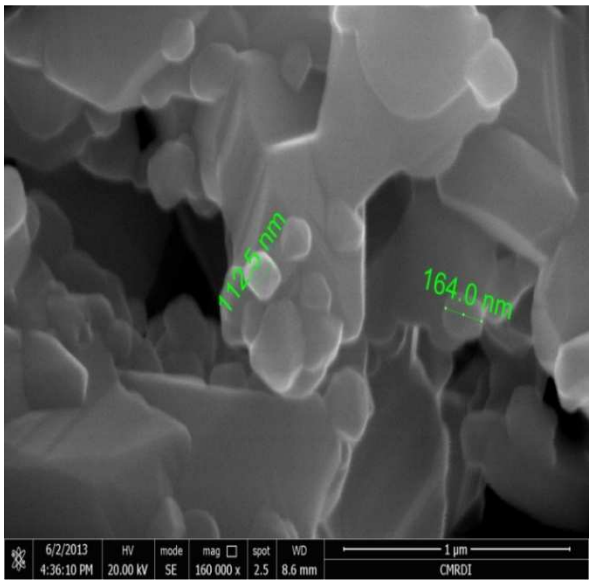

Fig. 5. *FESEM micrograph of the $Co_{0.8}Fe_{2.2}O_4$ annealed at 1000C°.*

3.2. Fourier Transform-Infra Red Spectroscopy

The FT-IR spectroscopy gives information about the local symmetry in the crystalline solids as the FT-IR spectra are sensitive to the short range of the oxygen co-ordination around the cations in both tetrahedral and octahedral clusters of the ferrites. It is predicted that two bands are observed in the region of 400–700cm^{-1} [30]. The one with the higher wave number,(υ_1), corresponds to the intrinsic stretching vibrations of the metal at the tetrahedral site and the second with the lower wave number (υ_2) corresponds to the intrinsic stretching vibration of the metal at the octahedral site.

The FT-IR in the range 400-4000cm^{-1} of the two systems under study are shown in Fig.6. In the case of $CoFe_2O_4$ (Fe/Co=2), there is two strong absorption bands at 605cm^{-1} (ν_1) and 417cm^{-1} (ν_2). The absorption bands observed in this range reveal the formation of single phase spinel structure having two sub lattices which are assigned to tetrahedral site at (ν_1) (M_{tet}) and octahedral site at (ν_2) (M_{oct}). The high wave number (ν_1) represents the vibration of Fe^{3+}- O^{2-} in the sub-lattice A-site, while the lower wave number band ν_2 represents the trivalent metal-oxygen vibrations at the octahedral B-sites. The absence of absorption bands between 700-4000cm^{-1} confirms the presence of no organic compound.

Similar results were published by other authors[21], however their results reported the splitting of these two bands. Recent FTIR data of $CoFe_2O_4$ synthesized using organic acid precursor method shows the presence of absorption bands at higher wave number aligned to the stretching mode of Co-O and C-H bands[25]. They attributed this to the insufficient time of calcinations to produce single phase of cobalt iron oxide.

With increasing the Fe/Co ratio to 2.72 the two main absorption bands at ν_1 and ν_2, nearly with the same intensity and area, are seen in the FTIR spectrum of the $Co_{0.8}Fe_{2.2}O_4$ system. However, ν_1 and ν_2 are shifted respectively to 597cm^{-1} and 507cm^{-1} and are still corresponding to M_{tet} and M_{oct} sites confirming the formation of metal oxides. The FTIR spectrum reveals also the presence of other absorption bands at 1663 and 3472cm^{-1}. These bands can be ascribed to the tensional stretching modes and H–O–H bending vibration of the free or absorbed water molecules[31,32]. It seems that increasing the Fe/Co content enhances the formation of such organic components.

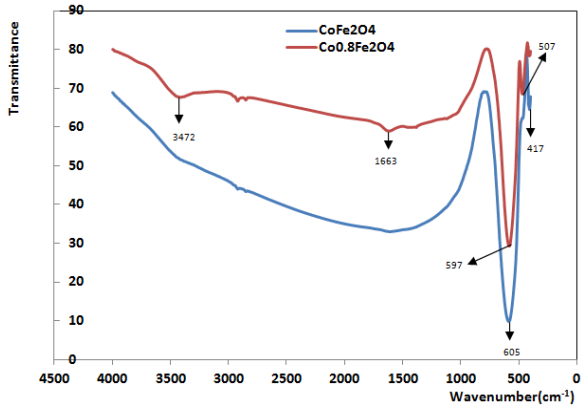

Fig. 6. *FT-IR spectra of $CoFe_2O_4$ and $Co_{0.8}Fe_{2.2}O_4$ annealed at 1000C°.*

3.3. Magnetization and Hystersis Loop Studies

Magnetic properties of the samples annealed at 1000C° were measured at room temperature under maximum applied field up to 20 kOe. The hysteresis loops are shown in Fig. 7 and the coercivity (Hc), saturation magnetization (Ms) and remanence ratio (Mr/Ms) were calculated and listed in Table 4. The saturation magntetization obtained was found to be 71.219emu/g for Fe/Co=2 and 55.635emu/g for Fe/Co=2.75. The values reported for M_S for the nano-systems under study are smaller than the bulk value (80emu/g). This result can be attributed to the nano sized cobalt ferrite particles in which the surface are larger and thus the surface energy and surface tension are high[33,34]. The change in M_S can be attributed to the change in crystallite size. As the single domain size of cobalt ferrite is reported to be around 50nm, the magnetization mechanism for the particle with size below and above the single domain size will be different ,which contributes to the variation observed in the coercivity values[25].

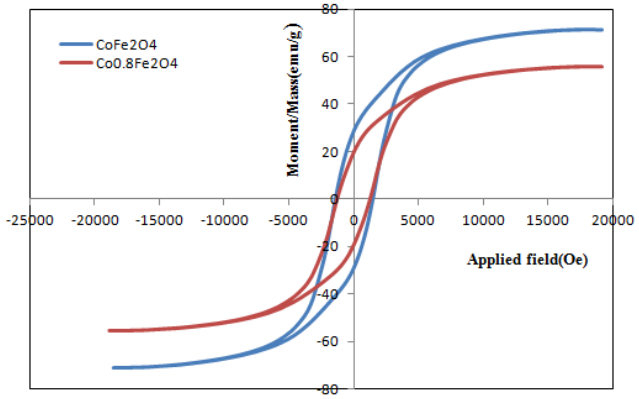

Fig. 7. *The hysteresis loops of the systems under study.*

The remanence ratios of the system under study are 0.405 and 0.349 for $CoFe_2O_4$ and $Co_{0.8}Fe_{2.2}O_4$ respectively. The value of remanence ratio of 0.405 is very close to that expected (0.5) for a system of non intracting single domain particles with uniaxial anisotropy even though cobalt ferrite itself has a cubic structure[35]. The existence of an effectively uniaxial anisotropy in magnetic nanoparticles has been attributed to surface effects as evidenced by simulations of nanoparticles[36].

Figure 8 shows the variation of magnetization of the two systems under study as a function of temperature. This figure shows that there is a gradual decrease in magnetization with temperature. It is assumed that the thermal energy helps the metal ions to overcome the energy barriers preventing an ordered cation distribution. Hence the inversion parameter decreases which results in the weakening of A–B exchange interaction, therefore, there is a fall in the magnetization value. The detected Curie temperatures (T_C) of $CoFe_2O_4$ for $Co_{0.8}Fe_{2.2}O_4$ are respectively 405C° and 410C°.

Table 4. displays the phase formation and the calculated magnetic parameters. As can be observed, increasing the Fe/Co ratio, in other words, increasing the hematite content and consequently decreasing the crystallite size results in remarkable decrease of the magnetic parameters. It seems that the stoichiometric ratio (Fe/Co of 2:1), probably, facilitates the exchange coupling interaction of crystals which will affect the magnetization reversal mechanisms.

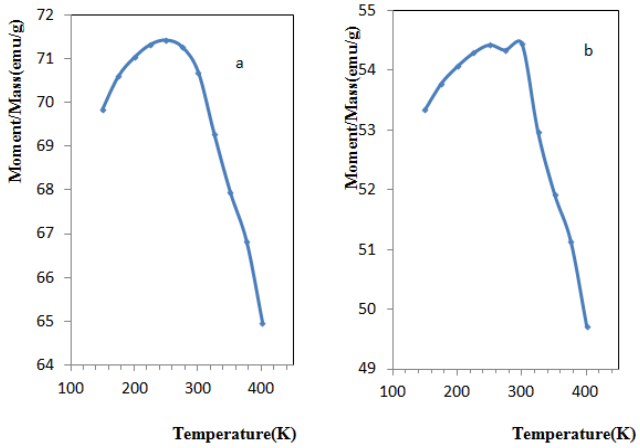

Fig. 8. *Plot of magnetization as a function of temperature (a) for $CoFe_2O_4$ and (b) for $Co_{0.8}Fe_{2.2}O_4$ annealed at 1000C°.*

Table 4. *The phase formation, the average $\mathcal{D}_\beta$ (nm) and the magnetic parametaress: M_s(emu/g), M_r(emu/g), M_r/M_s, H_C(Oe) T_C for the system under study.*

Sample	Phase formation	Average D_β (nm)	M_s emu/g	M_r emu/g	M_r/M_s	H_C Oe	T_C
$CoFe_2O_4$	3%	54.5	71.219	28.860	0.405	1443.8	405
$Co_{0.8}Fe_2O_4$	15%	48.6	55.635	19.453	0.349	1270.1	410

4. Conclusion

The role of annealing and Fe^{3+}/Co^{2+} ratio was investigated for co-precipitated $CoFe_2O_4$.

Increasing Fe^{3+}/Co^{2+} to 2.75% raised the formed second Fe_2O_3 phase to 15% at Ta=1000C.

The high Fe_2O_3 content decreased the crystallite size as displayed by WinFit program.

Crystallites agglomeration revealed by FESEM and H_2O detected by FTIR also occurred.

The values of Ms (71.219 emu/gm), Hc (Oe) and Mr/Ms decreased as detected by VSM.

References

[1] Y. Kitamoto, S. Kantake, F. Shirasaki, M. Abe, M. Naoe, J. Appl. Phys. 85(1999)4708.

[2] M. H. Sousa, F. A. Tourinho, J. Phys. Chem., B 105 (2001) 1168.

[3] Dennis E. Speliotis, J. Magn. Magn. Mater. 193 (1999) 29.

[4] Z. Ali, A. Atta, Y. Abbas, K. Sedeek, A. Adam, E. Abdetwab, J. thin solid films, xx (2014) xx

[5] P. C. Dorsey, P. Lubitz, K. B. Chrisey, J. S. Horwitz, J. Appl. Phys. 79 (1996) 6338.

[6] J. G. Lee, J. Y. Park, Y. J. Oh, C. S. Kimat Nanotech, Nanofabrication Facility at UC, Santa Barbara, 2003, pp. 106–107 , J. Appl. Phys. 84 (1998) 2801.

[7] A. K. Giri, K. Pellerin, W. Pongsaksawad, M. Sorescu, S. Majetich, IEEE Trans. Magn. 36 (2000) 3029.

[8] A. K. Giri, E. M. Kirkpatrick, P. Moongkhamklang, S. A. Majetich, Appl. Phys. Lett. 80 (2002) 2341.

[9] M. Grigorova, H. J. Blythe, V. Blaskov, V. Rusanov, V. Petkov, V. Masheva, D. Nihtianova, Ll. M. Martinez, J. S. Mu˜noz, M. Mikhov, J. Magn. Magn. Mater. 183 (1998) 163.

[10] J. L. Dorman, D. Fiorani (Eds.), Magnetic Properties of Fine Particles, North-Holland, Amesterdam, 1997.

[11] C. Inui, Y. Tsuge, H. Kura, S. Fujihara, S. Shiratori, T. Sato, Thin Solid Films 516 (2008) 2454.

[12] W. Zhao, J. Gu, L. Zhang, H. Chen, J. Shi, J. Am. Chem. Soc. 127 (2005) 8916.

[13] J. M. Perez, F. J. Simeone, A. Tsourkas, L. Josephson, R. Weissleder, Nano Lett. 4 (2004) 119.

[14] J. G. Na, T. D. Lee, S. J. Park, IEEE Trans. Magn. 28 (1992) 2433.

[15] C. C. H. Lo, A. P. Ring, J. E. Snyder, D. C. Jiles, IEEE Trans. Magn. 41(2005) 3676.

[16] Y. Köseoğlu, M. Bay, M. Tan, A. Baykal, H. Sözeri, R. Topkaya, N. Akdoğan, J. Nanopart. Res. 13 (2011) 2235.

[17] N. Kasapoğlu, A. Baykal, Y. Köseoğlu, M. S. Toprak, Scripta Mater. 57(2007) 441.

[18] H. Yang, X. Zhang, A. Tang, G. Qiu, Chem. Lett. 33 (7) (2004) 826.

[19] R. Honrada, R. Seshadri, A. Risbud, NNUN REU Program at nanotech, nanofabrication facility at UC, Santa Barbara, 2003, pp. 106-107.

[20] C. H. Chia, S. Zakaria, M. Yusoff, S. C. Goh, C. Y. Hawa, Sh. Ahmadi, N. M. Huang, H. N. Lim, J. Ceramics International 36 (2010) 605.

[21] Hamid Emadi, Ali Nemati Kharat, J. Industrial and Engineering Chemistry, xx (2014) xx.

[22] Sheenu Jauhar, SonalSinghal, Ceramics International 40(2014)11845.

[23] Yüksle Köseoğlu. Furkan Alan, Muhammed Tan, Resul Yilgin, Mustafa öztürk, J. Ceramics International 38 (2012) 3625.

[24] A. M. Al-Saie, M. Bououdina, A. Jaffar, S. Arekat, John M. Melnyczuk, Ynhi T. Thai, Christopher S. Brazel, J. Alloys and compounds 5095 (2011) 5393.

[25] R. M. Mohamed, M. M. Rashad, F. A. Haraz, W. Sigmund, J. Magnetism and Magnetic Materials, 322 (2010)2058.

[26] Ovidiu Caltun, Ioan Dumitru, Marcel Feder, Nicoleta Lupu, Haria Chiriac, J. Magn. Magn. Mater. 320 (2008) e869.

[27] P. Scardi, L. Lutterotti, and P. Masiterlli. Powder Diff. , 9(3) (1994)180.

[28] Karimat El-Sayed, Z. K. Heiba, K. Sedeek, H. H. Hantour, J. Alloys and compounds, 530 (2012) 102.

[29] Karimat El-Sayed, K. Sedeek, Z. K. Heiba, H. H. Hantour, J. Materials research bulletin, 48 (2013) 2383.

[30] R. D Waldron, Phys. Rev. 99(1955) 1727.

[31] Z. Karimi, Y. Mohammadifar, H. Shokrollahi , Sh. KhamenehAsl , Gh. Yousefi, L. Karimi J. Magn. Magn. Mater, 361(2014)150.

[32] I. Sharifi, H. Shokrollahi, J. Magn. Magn. Mater, 324(2012)2397.

[33] M. M. Rashad, R. M. Mohamed, H. El-Shall, J. Mater. Process. Technol. 198 (2008) 139.

[34] L. BenTahar, M. Artus, S. Ammar, L. S. Smiri, F. Herbst, M. -J. Vaulay, V. Richard, J. -M. Gren _eche, F. Villain, F. Fie´ vet, J. Magn. Magn. Mater. 320(2008)3242.

[35] D. H. Kim, D. E. Nikles, D. T. Johnson, C. S. Brazel, J. Magn. Magn. Mater. 320 (2008) 2390.

[36] M. Faraji, Y. Yamini, M. Rezaee, J. Iran. Chem. Soc. 7 (2010)1.